Analysis of stochastic resonance in coupled oscillator with fractional damping disturbed by polynomial dichotomous noise

Zhi Yan[1], Juan LG Guirao[2,3], T. Saeed[3], Huatao Chen[*1], Xianbin Liu[4]

[1] *Division of Dynamics and Control, School of Mathematics and Statistics, Shandong University of Technology, Zibo 255000, China*

[2] *Department of Applied Mathematics and Statistics, Technical University of Cartagena, Hospital de Marina, Cartagena 30203, Spain*

[3] *Department of Mathematics, Faculty of Science, King Abdulaziz University, P.O. Box 80203, Jeddah 21589, Saudi Arabia.*

[4] *State Key Laboratory of Mechanics and Control of Mechanical Structures, College of Aerospace Engineering, Nanjing University of Aeronautics and Astronautics, Nanjing 210016, China*

Abstract: Investigation on particle synchronization behavior and different kinds of stochastic resonance mechanism is reported in a fractional-order stochastic coupled system, which endures an external periodic excitation and polynomial asymmetric dichotomous noise damping disturbance. An extending of the method of stochastic averaging, the fractional Shapiro-Loginov formula and fractional Laplace transformation law are utilized, to determine the synchronization behavior between two coupled oscillators. The first moment of steady-state response and the output signal amplitude of the system are obtained in an analytical way, along with the stability condition. The crucial role of damping order and intrinsic frequency in stochastic resonance induced by noise intensity is explored, confirming the necessity of studying damping order falling in $(1,2)$. Due to the presence of nonlinear dichotomous colored noise, fresh phenomena of stochastic resonance and hypersensitive response induced by variation of external excitation frequency are found, where much more novel dynamical behaviors emerge than the non-disturbance case. It is confirmed that bimodal stochastic resonance only occurs for slow switching noise, with the damping order close to the parameter region of 0 or 2. For parameter-induced generalized stochastic resonance, explicit expressions of the critical damping strength corresponding to the optimal peak point of output amplitude are derived for the first time. By which different stochastic resonance patterns of the system under slow and fast switching noise perturbation are predicted successfully. In addition, the parametric effect and action mechanism of damping order on stochastic resonance are discussed in detail.

Keywords: Coupled stochastic system, Fractional order damping, Particle Synchronization behavior, Bona fide stochastic resonance, Generalized stochastic resonance

* Corresponding author.

E-mail addresses: yanzhi@sdut.edu.cn (ZY), juan.garcia@upct.es(JLG), htchencn@sdut.edu.cn(HC), xbliu@nuaa.edu.cn(XL).

1. Introduction

The concept of stochastic resonance (SR) was firstly proposed to explain the spectacle that the cycle of climate is consistent with that of the eccentric angle of the earth's revolution. Over the next 40 years, classical SR theories such as adiabatic dynamics[1], SR adiabatic elimination[2] and residence time distribution theory[3] were developed. And some scholars later proposed some new stochastic resonance theories such as super-threshold SR[4], which has been widely applied in different fields[5]. The occurrence of classical stochastic resonance must contain three essential elements, namely, system nonlinearity, periodic signal and random factor. While many studies have shown system nonlinearity is no longer a necessary condition, that SR can also occur in linear stochastic systems[6]. The difference is that the random factor in classical SR usually refers to additive white noise, while in linear stochastic system it can usually be induced by colored noise in multiplicative form[7].

Due to the premise that all physical quantities and dynamic evolution process can be represented respectively by integer-order operators and differential equations in classical mechanics category, most studies on SR were carried out for systems modeled by ODE. However, the integer order equation can only describe the instantaneous behavior at a certain moment, and the integer order operator is only a local quantity[8]. Based on the Markov process without aftereffect, classical stochastic resonance theory grounded on ordinary Langevin equation and FPE tends to be perfect gradually. However, with the development of natural science and industrial technology, more and more processes with memory effect have been discovered in the field of nature and engineering[9]. The current state of the process is often related to all historical states in the past, and modeling of ODE would be no longer applicable at this time[10]. As a non-local quantity[11], the characterization of fractional derivative involves the previous development course and the influence of non-local distribution, so it can be more accurate for such long-range or long-memory dependence process[12]. For instance, for soft materials which between elastic and viscous bodies, $\sigma(t) \propto \mathrm{d}^{\alpha}\varepsilon(t)/\mathrm{d}t^{\alpha}$, $0<\alpha<1$ is often used to describe the constitutive relation of viscoelastic materials[13]; Fractional convection-diffusion equations can be used to simulate some anomalous diffusion phenomena such as groundwater diffusion[14]; In some complex non-uniform medium environment[15], fractional derivative can be introduced to describe the memory damping force of the oscillator[16].

As a ubiquitous element in the real world and practical engineering systems, noise can induce many complex dynamic behaviors[17]. The constructive role of noise in SR has been extensively studied and explored in nearly a decade. However, due to the one-sided understanding of complex disturbances in many cases for the sake of convenient modeling, linear noise is used to simulate random factors in the system in practical applications, which is often not accurate enough[18]. In fact, nonlinear form noises exist more widely in real-world systems than the linear ones, some scholar has investigated the stochastic resonance in a linear system subjected to multiplicative noise that is a polynomial function of colored noise[19]. On the one hand, the noise in real systems is usually colored noise with limited bandwidth in spite of the fact that the Gaussian white noise (GWN) is simple and widely used in varies fields[20]. In the previous studies on SR of fractional order systems disturbed by color noise, most of the dichotomous and trichotomous colored noises usually exhibit as multiplicative form, to describe the mass disturbance, inherent frequency disturbance, signal modulation noise, etc. On the other hand, the above papers aim at the research on SR phenomenon in uncoupled stochastic systems, while particles in many stochastic systems are coupled, which is also called complex networks[21]. From the development of complex network in recent years and the gradual expansion of its application in various fields[22], one may sneak a peek at the practical research value of coupled stochastic fractional order system, and its SR related research will certainly have far-reaching significance and application value. As far as we know, there is no relevant reports on SR research for coupled fractional order systems with polynomial colored noise disturbance on fractional damping. Based on the above considerations, in this paper coupled fractional order systems with asymmetric dichotomous noise damping disturbances are considered, described as follows

$$\begin{cases} \ddot{z}_1(t) + [\delta + \Phi(\eta(t), N)]\, {}_C\mathrm{D}_{0,t}^q\, z_1(t) + \omega_0^{\,2} z_1(t) = \varepsilon(z_2 - z_1) + F\cos(\Omega t) \\ \ddot{z}_2(t) + [\delta + \Phi(\eta(t), N)]\, {}_C\mathrm{D}_{0,t}^q\, z_2(t) + \omega_0^{\,2} z_2(t) = \varepsilon(z_1 - z_2) + F\cos(\Omega t) \end{cases}. \tag{1.1}$$

The symbol “ δ ” in (1.1) represents the friction constant, and $\delta\, {}_C\mathrm{D}_{0,t}^q\, z_1(t)$ represents the fractional order damping, described in Caputo fractional derivative. According to the property of the damping materials[23], here the value of the fractional-order of a damping is selected in the interval $(0,2)$. In fact, many important results may be lost if we ignore the fractional-order value in the interval $(1,2)$ [24]. The fractional order item in (1.1) represents the extrinsic damping and internal damping force produced by the oscillator itself for $0 < q < 1$ and $1 < q < 2$, respectively. Here the fluctuation of the fractional damping strength is modeled by the random telegraph process[25], a simple but important type of non-white Markovian process $\eta(t)$, which has been adopted in some former works[26]. The polynomial function of the dichotomous noise $\Phi[\eta(t), N] = \sum_{k=1}^{N} \delta_k \eta^k(t)$ (with the positive integer $N \geq 2$) is actually responsible for the random friction of the oscillator, under effect of the changes in the nearby environment, which can be interpreted as an influx of energy to the oscillator and its dissipation to the surrounding environment. As the realization of two states Poisson process[27], in this paper the asymmetric dichotomous noise with two possible state values $\{\Delta_1, -\Delta_2\}$ are considered. The transition rate per unit of time from Δ_1 to $-\Delta_2$ is assumed as μ_1 and the transition rate of the reverse direction is μ_2, respectively. All the quantities Δ_1, $-\Delta_2$, μ_1 and μ_2 are positive, the transition probability of retention time at two states obeys Poisson distribution $\mu_{1,2}\exp(-\mu_{1,2}\tau_{1,2})$. Such a random switching process can be described by the following master equation[28]

$$\begin{aligned} \frac{\mathrm{d}}{\mathrm{d}t} P(\Delta_1, t \mid x, s) &= -\mu_1 P(\Delta_1, t \mid x, s) + \mu_2 P(-\Delta_2, t \mid x, s) \\ \frac{\mathrm{d}}{\mathrm{d}t} P(-\Delta_2, t \mid x, s) &= \mu_1 P(\Delta_1, t \mid x, s) - \mu_2 P(-\Delta_2, t \mid x, s) \end{aligned}, \tag{1.2}$$

$t > s$, with the initial condition $P(x', t \mid x, t) = \delta_{x'x}$, Eq. (1.2) can be solved as

$$\begin{aligned}P(\Delta_1, t \mid x, s) &= \frac{\mu_2}{\mu_1+\mu_2} + \left(\frac{\mu_1}{\mu_1+\mu_2}\delta_{\Delta_1 x} - \frac{\mu_2}{\mu_1+\mu_2}\delta_{-\Delta_2 x}\right)\exp\left[-(\mu_1+\mu_2)(t-s)\right] \\ P(-\Delta_2, t \mid x, s) &= \frac{\mu_1}{\mu_1+\mu_2} + \left(\frac{\mu_1}{\mu_1+\mu_2}\delta_{\Delta_1 x} - \frac{\mu_2}{\mu_1+\mu_2}\delta_{-\Delta_2 x}\right)\exp\left[-(\mu_1+\mu_2)(t-s)\right]\end{aligned} \quad (1.3)$$

For $t \to \infty$ steady-state solutions of (1.3) read

$$\begin{aligned}P_s(\Delta_1) &= \lim_{t\to\infty} P(\eta(t) = \Delta_1) = P(\Delta_1, \infty \mid x, s) = \frac{\mu_2}{\mu_1+\mu_2} \\ P_s(-\Delta_2) &= \lim_{t\to\infty} P(\eta(t) = -\Delta_2) = P(-\Delta_2, \infty \mid x, s) = \frac{\mu_1}{\mu_1+\mu_2}\end{aligned}, \quad (1.4)$$

from (1.4) the mean value and the autocorrelation function of $\eta(t)$ are given by

$$\begin{aligned}\langle \eta(t), t \mid x_0, s\rangle &= \sum_{x\in\{\Delta_1,-\Delta_2\}} xP(x,t \mid x_0, s) \\ &= \frac{\mu_2\Delta_1 - \mu_1\Delta_2}{\mu_1+\mu_2} + \left(x_0 - \frac{\mu_2\Delta_1 - \mu_1\Delta_2}{\mu_1+\mu_2}\right)\exp\left[-(\mu_1+\mu_2)(t-s)\right]\end{aligned}, \quad (1.5)$$

$$\begin{aligned}\langle \eta(t)\eta(s)\rangle &= \sum_{x_0, x_1\in\{\Delta_1,-\Delta_2\}} x_1 x_2 P(t, x_1 \mid s, x_0) P_s(x_0) \\ &= \left(\frac{\mu_2\Delta_1 - \mu_1\Delta_2}{\mu_1+\mu_2}\right)^2 + \frac{\mu_1\mu_2(\Delta_1+\Delta_2)^2}{(\mu_1+\mu_2)^2}\exp\left[-(\mu_1+\mu_2)(t-s)\right]\end{aligned}. \quad (1.6)$$

Let $t \to \infty$ in (1.5) one gets $\langle\eta\rangle_s = (\mu_2\Delta_1 - \mu_1\Delta_2)/(\mu_1+\mu_2) = 0$, inserting $\mu_2\Delta_1 - \mu_1\Delta_2 = 0$ into (1.6) leads to the variance $\mathrm{var}(\eta) = \mu_1\mu_2(\Delta_1+\Delta_2)^2/(\mu_1+\mu_2)^2 = \Delta_1\Delta_2$.

The transition probabilities between the two states from time s to t ($t > s$) are given as follows[29]

$$\begin{aligned}\left[P_{ij}(t-s)\right]_{i,j=1,2} &= \left[P\left(\eta(t) = (-1)^{j+1}\Delta_j \mid \eta(s) = (-1)^{i+1}\Delta_i\right)\right]_{i,j=1,2} \\ &= \begin{bmatrix} P_{11}(t-s) & P_{12}(t-s) \\ P_{21}(t-s) & P_{22}(t-s)\end{bmatrix} = \tau_{cor}\begin{bmatrix} \mu_2 + \mu_1 e^{-(t-s)/\tau_{cor}} & \mu_1\left(1 - e^{-(t-s)/\tau_{cor}}\right) \\ \mu_2\left(1 - e^{-(t-s)/\tau_{cor}}\right) & \mu_1 + \mu_2 e^{-(t-s)/\tau_{cor}}\end{bmatrix}\end{aligned}, \quad (1.7)$$

for $t - s \to \infty$ one can obtain the stationary probabilities of the asymmetric dichotomous process

$$P_s(\Delta_1) = \frac{\mu_2}{\mu_1+\mu_2}, \qquad P_s(-\Delta_2) = \frac{\mu_1}{\mu_1+\mu_2}. \quad (1.8)$$

With the presuppositions that statistical mean value is zero[30], i.e., $\Delta_1\mu_2 = \Delta_2\mu_1$, the autocorrelation function can be derived by (1.7) and (1.8)

$$\langle \eta(t)\eta(s)\rangle = \sum_{x_1, x_2\in\{\Delta_1,-\Delta_2\}} x_1 x_2 P(\eta(t) = x_2 \mid \eta(s) = x_1) P_s(x_1) = \sigma e^{-\nu(t-s)} = \frac{D}{\tau_c} e^{-\nu(t-s)}. \quad (1.9)$$

Where $\sigma = \Delta_1\Delta_2$, $\nu = \mu_1 + \mu_2$ is the switching rate of $\eta(t)$, the intensity of the dichotomous noise is defined as, $D = \int_0^\infty \langle \eta(t)\eta(t+u)\rangle \mathrm{d}u = \sigma/\nu$ and the correlation time can also be calculated as $\tau_c = \int_0^\infty \langle \eta(t)\eta(t+u)\rangle u\mathrm{d}u / D = 1/\nu$. With the constructed equation $(\eta - \Delta_1)(\eta + \Delta_2) = 0$, one gets $\eta^2 = \sigma + \Lambda\eta$, $\eta^3 = \sigma\Lambda + (\sigma + \Lambda)\eta$, $\eta^k = \alpha_k\eta + \beta_k$ with $\alpha_k = \left[\Delta_1^{\,k} - (-\Delta_2)^k\right]/(\Delta_1 + \Delta_2)$, $\beta_k = \left[\Delta_2\Delta_1^{\,k} + \Delta_1(-\Delta_2)^k\right]/(\Delta_1 + \Delta_2)$. $\Lambda = \Delta_1 - \Delta_2$ denotes the asymmetry between the two states.

For arbitrary integer k, the polynomial function of $\eta(t)$ can be rewritten as

$$\Phi(\eta(t),N)=\sum_{k=1}^{N}\delta_k\eta^k(t)=\sum_{k=1}^{N}\delta_k\alpha_k\eta(t)+\sum_{k=1}^{N}\delta_k\beta_k\,. \tag{1.10}$$

For convenience sake, let $E_\alpha=\sum_{k=1}^{N}\delta_k\alpha_k$, $E_\beta=\sum_{k=1}^{N}\delta_k\beta_k$, then the original Eq. (1.1) reads:

$$\begin{cases}\ddot{z}_1(t)+[\delta+E_\alpha\eta(t)+E_\beta]\,{}_C\mathrm{D}^q_{0,t}\,z_1(t)+\omega_0^{\,2}z_1(t)=\varepsilon(z_2-z_1)+F\cos(\Omega t)\\ \ddot{z}_2(t)+[\delta+E_\alpha\eta(t)+E_\beta]\,{}_C\mathrm{D}^q_{0,t}\,z_2(t)+\omega_0^{\,2}z_2(t)=\varepsilon(z_1-z_2)+F\cos(\Omega t)\end{cases}, \tag{1.11}$$

the subscripts 'C' and '0, t' in the fractional derivative symbol has been dropped for notational convenience.

Different kinds of stochastic resonance of system (1.11) are investigated, the major factors affecting the synchronous speed of the two coupled oscillators are demonstrated from both qualitative and quantitative angle. By which, complexity induced by the nonlinear telegraphic noise and the mechanical mechanism of synchronization and resonance regimes will be elaborated. The structure of this paper is as follows. In sec. II the averaging synchronization between particle z_1 and z_2 are demonstrated from theoretical and numerical angle, respectively. Section III is devoted to quantify the steady-state output amplitude and the response first moment of the system. Based on which, in Section IV phenomena of traditional SR induced by noise intensity, Bona fide SR induced by external excitation frequency and GSR induced by different system parameters are discussed in detail. Section V presents the main results and conclusions of this paper.

2. Synchronization behavior and verification

Before going into the underlying resonant behavior in the coupled oscillators described by Eq. (1.11), the synchronism between each particle of (1.11) should be firstly examined, say, to verify whether or not the average behaviors of z_1 is consistent with z_2 in the long-time regime[31]. To this end, we examine the synchronization[32] by introducing the symbol of mean field $z=(z_1+z_2)/2$.

2.1. Theoretical prediction of synchronization

Firstly, rewrite Eq. (1.11) in the following expression:

$$\ddot{z}_k+\left[\delta+E_\alpha\eta+E_\beta\right]\mathrm{D}^q\,z_k+\omega_0^{\,2}z_k=\varepsilon\sum_{j=1}^{2}(z_j-z_k)+F\cos(\Omega t)\,,\quad k=1,2\,. \tag{2.1}$$

The deviations of z_k ($k=1,2$) to z is given by $B_k(t)=z_k(t)-z(t)$.

Calculating the summation of the two single movement equation of the particle in Eq. (2.1) to estimate that of the mean field

$$\ddot{z}+\left[\delta+E_\alpha\eta+E_\beta\right]\mathrm{D}^q\,z+\omega_0^{\,2}z=F\cos(\Omega t)\,. \tag{2.2}$$

From Eq. (2.1) and (2.2) the equivalent equations for the deviation function B_k is given by

$$\ddot{B}_k+\left[\delta+E_\alpha\eta+E_\beta\right]\mathrm{D}^q\,B_k+\omega_0^{\,2}B_k=\varepsilon\sum_{j=1}^{2}\left(B_j-B_k\right),\quad k=1,2\,. \tag{2.3}$$

Taking average of the two equations in (2.3), one gets

$$\begin{cases}\left(\dfrac{\mathrm{d}^2}{\mathrm{d}t^2}+\omega_0^{\ 2}+\varepsilon\right)\langle B_1\rangle+\left[\delta+E_\beta\right]\mathrm{D}^q\langle B_1\rangle+E_\alpha e^{-vt}\,\mathrm{D}^q\left(\langle\eta B_1\rangle e^{vt}\right)-\varepsilon\langle B_2\rangle=0\\ \left(\dfrac{\mathrm{d}^2}{\mathrm{d}t^2}+\omega_0^{\ 2}+\varepsilon\right)\langle B_2\rangle+\left[\delta+E_\beta\right]\mathrm{D}^q\langle B_2\rangle+E_\alpha e^{-vt}\,\mathrm{D}^q\left(\langle\eta B_2\rangle e^{vt}\right)-\varepsilon\langle B_1\rangle=0\end{cases},\tag{2.4}$$

B_k can be regarded as a function of $\eta(t)$, due to exponential correlation property of the concerned random noise $\eta(t)$, the famous Shapiro-Loginov formula[33] can be explored

$$\left\langle\eta(t)\frac{\mathrm{d}}{\mathrm{d}t}B_k(t)\right\rangle=\frac{\mathrm{d}}{\mathrm{d}t}\langle\eta(t)B_k(t)\rangle+v\langle\eta(t)B_k(t)\rangle.\tag{2.5}$$

Reuse the typical formula (2.5) twice to give the corresponding averaging results for the two-order differential of a function of exponential correlation random noise:

$$\left\langle\eta(t)\frac{\mathrm{d}^2}{\mathrm{d}^2 t}B_k(t)\right\rangle=\frac{\mathrm{d}^2}{\mathrm{d}^2 t}\langle\eta(t)B_k(t)\rangle+2v\frac{\mathrm{d}}{\mathrm{d}t}\langle\eta(t)B_k(t)\rangle+v^2\langle\eta(t)B_k(t)\rangle,\tag{2.6}$$

the extended generalized fractional Shapiro-Loginov formulas can also be derived by Eq. (2.5) and the definition of Caputo derivative, which has been utilized in Eq. (2.7)

$$\langle\eta(t)\,\mathrm{D}^q B_k(t)\rangle=e^{-vt}\,\mathrm{D}^q\left(\langle\eta(t)B_k(t)\rangle e^{vt}\right),\ \ k\in\{1,2\}.\tag{2.7}$$

The synthetic affections of the mean-value $\langle\eta B_k\rangle$ $k=1,2$ appear in (2.4), to address the new term and obtain both the two variables together, we should multiply Eq. (2.2) with $\eta(t)$ and conduct the averaging operation again to get the following equation:

$$\begin{cases}\left[\left(\dfrac{\mathrm{d}}{\mathrm{d}t}+v\right)^2+\omega_0^{\ 2}+\varepsilon\right]\langle\eta B_1\rangle+\left[\delta+E_\beta+\Lambda E_\alpha\right]e^{-vt}\,\mathrm{D}^q\left(\langle\eta B_1\rangle e^{vt}\right)+E_\alpha\sigma\,\mathrm{D}^q\langle B_1\rangle-\varepsilon\langle\eta B_2\rangle=0\\ \left[\left(\dfrac{\mathrm{d}}{\mathrm{d}t}+v\right)^2+\omega_0^{\ 2}+\varepsilon\right]\langle\eta B_2\rangle+\left[\delta+E_\beta+\Lambda E_\alpha\right]e^{-vt}\,\mathrm{D}^q\left(\langle\eta B_2\rangle e^{vt}\right)+E_\alpha\sigma\,\mathrm{D}^q\langle B_2\rangle-\varepsilon\langle\eta B_1\rangle=0\end{cases}.\tag{2.8}$$

In the calculation of Eq. (2.8) we have used the averaging formula (2.6) and (2.7) simultaneously. The collection of (2.4) and (2.8) truly consist a close linear system of second-order differential equations for four variables, i.e., $x_1=\langle B_1\rangle$, $x_2=\langle B_2\rangle$, $x_3=\langle\eta B_1\rangle$ and $x_4=\langle\eta B_2\rangle$. Since the solutions in long-time region is where our focus should be, the stationary region where the initial conditions impact on the long-time limit behavior should be experientially empirically omitted. By virtue of the Laplace transform technique, this equation set can be equivalently changed to the corresponding linear algebraic equation set in (2.9)

$$\begin{cases}a_{11}X_1(s)+a_{12}X_2(s)+a_{13}X_3(s)=0\\ a_{21}X_1(s)+a_{22}X_2(s)+a_{24}X_4(s)=0\\ a_{31}X_1(s)+a_{33}X_3(s)+a_{34}X_4(s)=0\\ a_{42}X_2(s)+a_{43}X_3(s)+a_{44}X_4(s)=0\end{cases},\tag{2.9}$$

where $X_i(s)=\mathrm{L}\{x_i(t);s\}$, $i=1,2,3,4$, expressions of coefficients in Eq. (2.9) are given by

$a_{11}=s^2+\omega_0^2+\varepsilon+\left(\delta+E_\beta\right)s^q$, $a_{12}=-\varepsilon$, $a_{13}=E_\alpha$, $a_{21}=a_{12}$, $a_{22}=a_{11}$, $a_{24}=a_{13}$, $a_{31}=\sigma E_\alpha s^q$, $a_{33}=\left(s+v\right)^2+\omega_0^2+\varepsilon+\left(\delta+E_\beta+\Lambda E_\alpha\right)\left(s+v\right)^q$, $a_{34}=a_{12}$, $a_{42}=a_{31}$, $a_{43}=a_{12}$, $a_{44}=a_{33}$.

Equations (2.9) lead to $X_i(s)=0$, according to the inverse Laplace transform theory, we have $\langle B_1\rangle=\langle B_2\rangle=0$, which reveals that the average value of the displacement of each particle is agreement with that of the mean one. Moreover, $\langle z_1\rangle=\langle z_2\rangle$ and the synchronization behavior of this two-coupled oscillators under arbitrary order polynomial asymmetric dichotomous noise has been confirmed. In summary, synchronization behavior happens in the two coupled system, by which, one just need to estimate the single degree (e.g., z_1) to investigate the overall stationary-state behavior of the coupled system. In next Section the synchronization will be invested to give the analysis of the SR phenomenon.

2.2. Numerical verification

In terms of numerical simulation scheme, there are many approximate discrete methods for the fractional derivative operator $\mathrm{D}^q B_k$ in Eq. (2.3). The G-L approximation approach is considered to be the most straightforward one from the numerical implementation point of view, and has been widely adopted in problems in dealing with fractional-order issues for its simplicity in the discretization scheme angle. The specific expression is as follows

$$[{}_{GL}\mathrm{D}_{t_0,t}^q f(t)]_{t=t_n}=\Delta t^{-q}\sum_{j=0}^{n+p}(-1)^j\binom{q}{j}f(t_n-t_j+p)\,, \tag{2.10}$$

this formula is referred to the *standard G-L formula* and *right shifted G-L formula* for $p>0$, respectively. Wherein the shift parameter p is a positive integer, $t_j{=}j\Delta t$, $j=1,2,\ldots$, while (2.10) provides only the first-order accuracy for smooth function $f(t)$ if $f(0)=0$. Numerical iteration algorithm based on (2.10) in previous works are obtained under the homogeneous initial condition assumption, which can not be applied in the situation with arbitrary initial condition. As a comparison, algorithm based on the Caputo definition derivative is adaptive for nonhomogeneous initial condition situation[34]. Moreover, the R–L derivative coincides with the G–L one for a wide class of functions in real physical and engineering applications, if suitable smoothness conditions are satisfied. While R-L definition leads to initial conditions concerning the limit values of fractional derivatives which have no known certain physical meaning, resulting in practical difficulties appearing in engineering application, this awkward situation will not occur for Caputo derivative[35]. To obtain the numerical verification of the collective synchronization behavior, here one simulation based on the Caputo derivative definition is adopted. When two types of fractional Caputo derivatives with q falling into $(0,1)$ and $(1,2)$, the discretization method is desired by the L1 and L2 approximation approaches, respectively[36]. Specifically, $t_0{=}0$ without loss of generality and definiteness, let $t_0{=}0$, $t_n{=}n\Delta t$, then for $0<q<1$

$$\begin{aligned}[{}_C\mathrm{D}_{0,t}^q f(t)]_{t=t_n}&\approx\frac{1}{\Gamma(1-q)}\sum_{j=0}^{n-1}\frac{f(t_{j+1})-f(t_j)}{\Delta t}\int_{t_j}^{t_{j+1}}(t_n-s)^{-q}\,\mathrm{d}s\,,\\&=\begin{cases}\aleph_0 f(t_n)-\aleph_{n-1}f(t_0)+\sum_{j=1}^{n-1}(\aleph_{n-j}-\aleph_{n-j-1})(f(t_j)) & n\ge 2\\ \aleph_0 f(t_1)-\aleph_0 f(t_0) & n=1\end{cases},\end{aligned} \tag{2.11}$$

where $\aleph_j=[(j+1)^{1-q}-j^{1-q}]/[\Gamma(2-q)\Delta t^q]$, $j=1,2,\ldots$.

For $1<q<2$, the approximation approach reads

$$\left[{}_{C}\mathrm{D}_{0,t}^{q} f(t)\right]_{t=t_n} = \frac{1}{\Gamma(2-q)}\sum_{j=0}^{n-1}\int_{t_j}^{t_{j+1}}(t_n-s)^{1-q} f''(s)\,\mathrm{d}s \approx \sum_{j=-1}^{n}\Im_j(f(t_{n-j})), \tag{2.12}$$

with $$\Im_j = \frac{1}{\Gamma(3-q)\Delta t^q}\begin{cases} 1 & j=-1 \\ 2^{2-q}-3 & j=0 \\ (j+2)^{2-q}-3(j+1)^{2-q}+3j^{2-q}-(j-1)^{2-q} & 1\le j\le n-2 \\ -2n^{2-q}+3(n-1)^{2-q}-(n-2)^{2-q} & j=n-1 \\ n^{2-q}-(n-1)^{2-q} & j=n \end{cases}.$$

For $q=1$, Eq. (1.1) is reduced to the ordinary equation and of course one can employ the fourth-order Runge-Kutta algorithm[37] to provide an approximation with sufficient precision, otherwise Eq. (2.3) can be rewritten in the following way:

$$\begin{cases} \dot{B}_k = \vartheta_k \\ \dot{\vartheta}_k + \left[\delta + E_\alpha \eta + E_\beta\right]\mathrm{D}^q B_k + \omega_0{}^2 B_k = \varepsilon\sum_{j=1}^{2}\left(B_j - B_k\right) \end{cases} \quad k=1,2, \tag{2.13}$$

substituting (2.11) and (2.12) into (2.13) one gets

$$\begin{cases} B_k(n+1) = B_k(n) + \Delta t\vartheta_k \\ \vartheta_k(n+1) = \vartheta_k(n) + \Delta t\left\{-\left[\delta + E_\alpha\eta(n) + E_\beta\right]D_n - \omega_0{}^2 B_k(n) + \varepsilon\sum_{j=1}^{2}\left(B_j(n) - B_k(n)\right)\right\} \end{cases}, \tag{2.14}$$

$$D_n = \left[D_{0,t}^{q} B_k(t)\right]_{t=t_n} = \begin{cases} \sum_{j=0}^{n-1}\aleph_{n-j-1}(B_k(t_{j+1}) - B_k(t_j)) & 0<q<1 \\ \sum_{j=-1}^{n}\Im_j(B_k(t_{n-j})) & 1<q<2 \end{cases}, \tag{2.15}$$

with $B_k(n) = B_k(t_n)$, $\vartheta_k(n) = \vartheta_k(t_n)$, $k=1,2$, $\eta(n) = \eta(t_n)$.

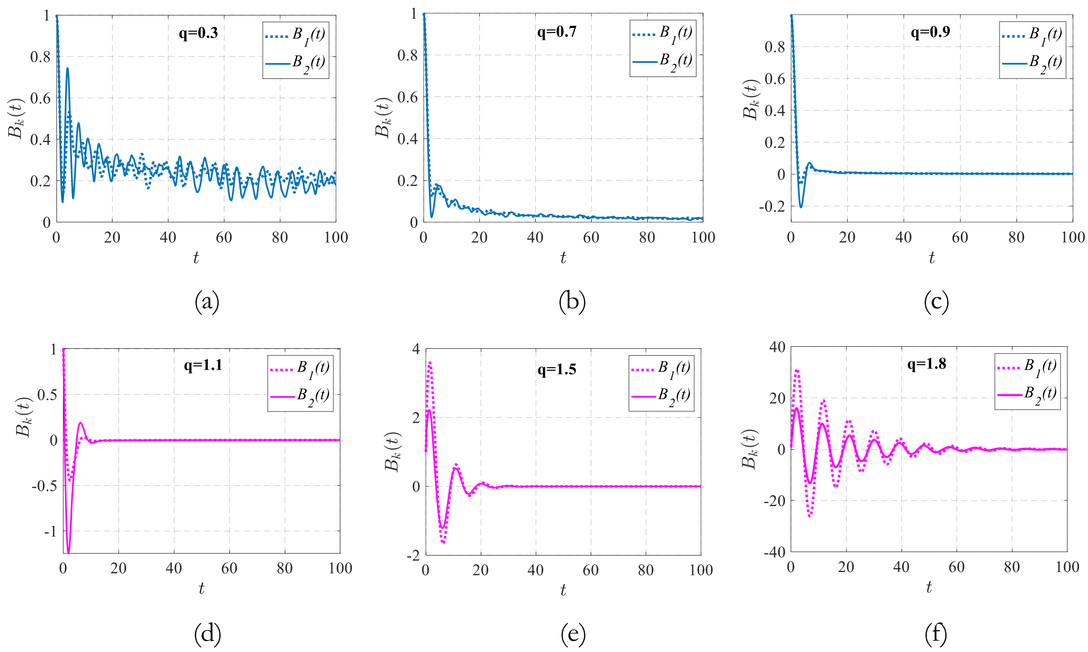

Fig. 1. (Color online) Numerical simulation realization of kth particle deviation $B_k(t)$ with different fractional damping order.

Considering two states of the dichotomous noise as $\Delta_1 = 1.2$, $\Delta_2 = 0.6$ under correlation time $\tau_{cor} = 0.1$, system parameters are set to $\varepsilon = 0.8$, $\delta = 1$, $E_\alpha = 0.5$, $E_\beta = 0.2$, $\omega_0^2 = 1$. In Fig. 1 numerical results of the convergence of *k*th particle $B_k(t)$ under different fractional order q with the initial condition $z_k(0) = 1$. It can be seen that the deviation function $B_k(t)$ always converge to 0 under long-term limit situation, that is to say, the movement of both the two coupled particles exhibit uniform behavior and tend to the mean field $z(t)$. For the case of $q < 1$, a comparison of Fig 1(a-c) reveals that the speed of synchronization of two particles exhibits an evidently increasing with the fractional order q approaching to 1. While the situation is opposite for the case of $q > 1$, from $q = 1.1$ to $q = 1.8$, the synchronization of the two particles takes more and more time as q increases. These two phenomena can be explained as follows: When the fractional damping order q approaching to 1, the memory effect of the system exhibit more and more inconspicuous[32]. At this time, the damping force represented by the integral of the memory kernel function tends to be smaller, leading to a faster synchronization speed of particles on the two DOF. On the contrary, when the damping order is too small or too large, memory effect is prominent so that the damping force is obvious, so the two particles need longer time to accomplish synchronization. Fig. 2 shows the influence of parameters E_α and D on the synchronization velocity of two particles, it is determined that neither noise parameters nor noise intensity can exert influence on synchronous speed.

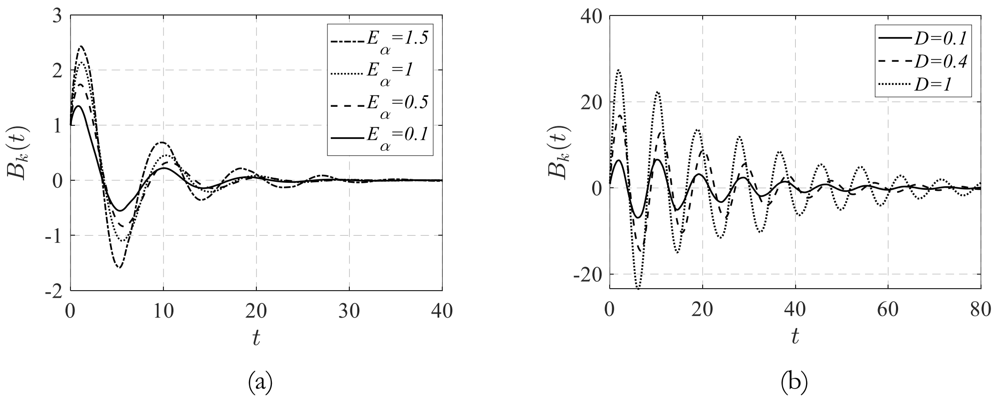

Fig. 2. (a) Effect of coefficient E_α the particle deviation $B_k(t)$ with $q = 1.5$; (b) Effect of noise intensity D on particle deviation $B_k(t)$ with $q = 1.8$.

3. Analysis of steady-state response

To investigate the potential resonant behavior hidden within the system described by Eq. (1.1), it is necessary to estimate the spectral amplification (SPA) of the oscillator, despite that there are several other alternative assessment indexes to quantify the SR phenomenon[38]. To this end, the mean value of the displacement of the oscillator should be obtained analytically before discussing the SR behavior in the system. In this section the steady-state response will be discussed in detail, after that the analytical results of SPA will be gotten by utilizing the stochastic averaging method, typical and extended fractional Shipiro-Loginov formulas.

Due to the perfectly identify movement pattern between $z_1(t)$ and $z_2(t)$ which has been confirmed in Section II, one just need to calculate the first-order moment of the mean field $\langle z(t)\rangle$ to indicate the average of each particle $\langle z_k(t)\rangle$. Indeed, in section II the synchronization manner between z_1 and z_2 has given the assertion that the deviations of the mean field of the two particles will tend to 0 in long-time limit, i.e., $\langle z(t)-z_{1,2}(t)\rangle \xrightarrow{t\to\infty} 0$. The calculation of the exact solution of the first-order moment is feasible since the displacement process $\langle z_k(t)\rangle$ could be always stationary[39]. In fact, the fractional particle in Eq. (1.1) will always be dragged back to the origin sooner or later thanks to the harmonic potential $V(t)=\omega_0^2 z_k^2/2$.

To obtain the analytical solution of $\langle z(t)\rangle$ we first take average of Eq. (2.2) and use the fractional Shapiro-Loginov formula (2.7), to gain

$$\left(\frac{\mathrm{d}^2}{\mathrm{d}t^2}+\omega_0^2\right)\langle z\rangle+\left[\delta+E_\beta\right]\mathrm{D}^q\langle z\rangle+E_\alpha e^{-vt}\,\mathrm{D}^q\left(\langle\eta z\rangle e^{vt}\right)=F\cos(\Omega t), \tag{3.1}$$

another equation is required to give rise to the solution of the new emerged term $\langle\eta z\rangle$. For this purpose, multiplying Eq. (2.2) by η, averaging all the terms on both sides of the gained equation, one gets

$$\langle\eta\ddot{z}\rangle+\left(\delta+E_\beta\right)\langle\eta\,\mathrm{D}^q z\rangle+E_\alpha\langle\eta^2\,\mathrm{D}^q z\rangle+\omega_0^2\langle\eta z\rangle=0, \tag{3.2}$$

considering the relevant properties $\eta^2=\sigma+\Lambda\eta$ and inserting the Shapiro-Loginov formulars given by (2.6), (2.7) into Eq. (3.2), the equation can be rewritten as

$$\left[\left(\frac{\mathrm{d}}{\mathrm{d}t}+v\right)^2+\omega_0^2\right]\langle\eta z\rangle+\left(\delta+\Lambda E_\alpha+E_\beta\right)e^{-vt}\,\mathrm{D}^q\left(\langle\eta z\rangle e^{vt}\right)+E_\alpha\sigma\,\mathrm{D}^q\langle z\rangle=0. \tag{3.3}$$

The collection of Eqs. (3.1), (3.3) truly constitute one close linear system of second-order differential equations in regard to variables $x_1=\langle z\rangle$ and $x_2=\langle\eta z\rangle$

$$\begin{cases}\left(\dfrac{\mathrm{d}^2}{\mathrm{d}t^2}+\omega_0^2\right)x_1+\left[\delta+E_\beta\right]\mathrm{D}^q x_1+E_\alpha e^{-vt}\,\mathrm{D}^q\left(x_2e^{vt}\right)=F\cos(\Omega t)\\ \left[\left(\dfrac{\mathrm{d}}{\mathrm{d}t}+v\right)^2+\omega_0^2\right]x_2+\left(\delta+\Lambda E_\alpha+E_\beta\right)e^{-vt}\,\mathrm{D}^q\left(x_2e^{vt}\right)+E_\alpha\sigma\,\mathrm{D}^q x_1=0\end{cases}. \tag{3.4}$$

By virtue of the Laplace transform technique [40], the Laplace transformation of q-order fractional derivative of a function $f(t)$ with proper smoothness can be given by

$$\mathrm{L}\left\{\mathrm{D}^q\left[f(t)\right],s\right\}=s^q\tilde{f}(s)-\sum_{k=0}^{\lceil q\rceil-1}s^{q-k-1}f^{(k)}(0). \tag{3.5}$$

Wherein $\tilde{f}(s)$ is the Laplace transform of $f(t)$: $\tilde{f}(s)=\mathrm{L}\{f(t),s\}=\int_0^\infty e^{-st}f(t)\mathrm{d}t$, $f^{(k)}(0)$ denotes the initial values "$\lceil q\rceil$" denotes the fractional value q rounded up to the nearest integer, e.g. $\lceil q\rceil=1$ and $\lceil q\rceil=2$ for $0<q\le 1$ and $1<q<2$, respectively. When put in mind of the translation theorem, one can further get

$$\begin{aligned}L\left\{e^{-kvt}\mathrm{D}^q\left[f(t)e^{kvt}\right],s\right\}&=(s+kv)^q\,\tilde{f}(s)-(s+kv)^{q-1}f(0)\\&\quad-(s+kv)^{q-2}\left[f'(0)+kvf(0)\right]\delta_{n_1n_2}\end{aligned}. \tag{3.6}$$

In (3.6) δ is the Dirichlet function with $n_1 = 2$ and $n_2 = \lceil q \rceil$, the last term vanishes and it exist for the fractional order of the damping greater than 1. The usage of formulars (3.5) and (3.6) makes it doable that (3.4) can further be equivalently changed to a corresponding linear algebraic equation set

$$\begin{cases} a_{11}X_1 + a_{12}X_2 = Fs\big/\left(s^2+\Omega^2\right) + c_{11}x_1(0) + c_{12}x_2(0) + d_{11}x_1'(0) + d_{12}x_2'(0) \\ a_{21}X_1 + a_{22}X_2 = c_{21}x_1(0) + c_{22}x_2(0) + d_{21}x_1'(0) + d_{22}x_2'(0) \end{cases}, \tag{3.7}$$

with the coefficients in (3.7) given as follows

$a_{11} = s^2 + \omega_0^2 + \left(\delta + E_\beta\right)s^q$, $a_{12} = E_\alpha\left(s+v\right)^q$, $a_{21} = \sigma E_\alpha s^q$,

$a_{22} = \left(s+v\right)^2 + \omega_0^2 + \left(\delta + \Lambda E_\alpha + E_\beta\right)\left(s+v\right)^q$, $c_{11} = s + \left(\delta + E_\beta\right)s^{q-1}$,

$c_{12} = E_\alpha\left(s + v + v\delta_{n_1 n_2}\right)\left(s+v\right)^{q-2}$, $c_{21} = \sigma E_\alpha s^{q-1}$,

$c_{22} = s + 2v + \left(\delta + \Lambda E_\alpha + E_\beta\right)\left(s + v + v\delta_{n_1 n_2}\right)\left(s+v\right)^{q-2}$

$d_{11} = 1 + \left(\delta + E_\beta\right)s^{q-2}\delta_{n_1 n_2}$, $d_{12} = E_\alpha\left(s+v\right)^{q-2}\delta_{n_1 n_2}$,

$d_{21} = \sigma E_\alpha s^{q-2}\delta_{n_1 n_2}$, $d_{22} = 1 + v\left(\delta + \Lambda E_\alpha + E_\beta\right)\left(s+v\right)^{q-2}\delta_{n_1 n_2}$

$X_k(s) = \mathrm{L}\left\{x_k(t), s\right\}$, $k = 1, 2$, $x_k(t)$ and $x_k'(t)$ represent the initial conditions. In order to get the analytical results of the first-order moment, one should firstly calculate the solution of $X_1(s)$ by solving (3.7)

$$X_1(s) = \hat{G}_{10}(s)\frac{Fs}{s^2+\Omega^2} + \sum_{k=1}^{2}\hat{G}_{1k}(s)x_k(0) + \sum_{k=1}^{2}\hat{I}_{1k}(s)x_k'(0), \tag{3.8}$$

where the transformed functions in Eq. (3.8) are completely determined by a_{kl}, c_{kl} and d_{kl}, $k, l \in \{1, 2\}$, which are expressed as follows:

$$\hat{G}_{10}(s) = \frac{a_{22}}{a_{11}a_{22} - a_{12}a_{21}},\ \hat{G}_{11}(s) = \frac{c_{11}a_{22} - a_{12}c_{21}}{a_{11}a_{22} - a_{12}a_{21}},\ \hat{G}_{12}(s) = \frac{c_{12}a_{22} - a_{12}c_{22}}{a_{11}a_{22} - a_{12}a_{21}},$$

$$\hat{I}_{11}(s) = \frac{d_{11}a_{22} - a_{12}d_{21}}{a_{11}a_{22} - a_{12}a_{21}},\ \hat{I}_{12}(s) = \frac{d_{12}a_{22} - a_{12}d_{22}}{a_{11}a_{22} - a_{12}a_{21}}.$$

It should be noted that $X_2(s)$ can also be solved and be expressed in an analogous way to that of (3.8), while it is not necessary to discuss here when the mean value $\langle z \rangle$ is the only point of interest. Now using the inverse Laplace transform method on the expression (3.8) and considering the relevant unicity theorem[41], one can get the solution of the first-order moment value of the mean field $\langle z \rangle$, represented in the following form:

$$\langle z(t) \rangle = G_{10}(t) * \left[F\cos(\Omega t)\right] + \sum_{k=1}^{2}G_{1k}(t)x_k(0) + \sum_{k=1}^{2}I_{1k}(t)x_k'(0), \tag{3.9}$$

with $G_{10}(t) = \mathrm{L}^{-1}\left\{\hat{G}_{10}(s)\right\}$, $G_{1k}(t) = \mathrm{L}^{-1}\left\{\hat{G}_{1k}(s)\right\}$, $I_{1k}(t) = \mathrm{L}^{-1}\left\{\hat{I}_{1k}(s)\right\}$, in (3.9) the asterisk denotes the convolution operator.

According to the theory of the stability condition[42] the stability of the solution (3.9) could be guaranteed under the circumstances that all the possible solutions of the equation $a_{11}a_{22}-a_{12}a_{21}=0$ have roots with a negative or zero real part.

$$v^2+\omega_0^{\ 2}+\left(\delta+\Lambda E_\alpha+E_\beta\right)v^q>0\,. \tag{3.10}$$

Meanwhile, considering the asymptotic behavior of $\langle z(t)\rangle$ given in the expression (3.9), again, applying the Tauberian theorem[43] in the functions on the right side of Eq. (3.9) gives the approximation for $t\to\infty$: $G_{10}(t)\to O(t^{-q})$ and $G_{1k}(t)$, $I_{1k}(t)\to O(t^{-q-1})$, thus the memorizing effect of the initial conditions $x_k(0)$, $x_k'(0)$, $k=1,2$, should be ignored. Accordingly, the averaging value of the mean field displacement in the long-time limit regime can be given by

$$\langle z(t)\rangle_{as}=F_0\int_0^t G_{10}(t-t')\cos(\Omega t')\,\mathrm{d}\,t'\,. \tag{3.11}$$

Making use of the linear response result based on the theory of signal and system[44], when a linear system is inputted by a periodic signal $F\cos(\Omega t)$, the output signals of this system will still keep as a harmonic signal, with a same period and a phase skewing

$$\langle z(t)\rangle_{as}=S\cos(\Omega t+\vartheta)\,. \tag{3.12}$$

Due to the form of the expression of $\langle z(t)\rangle$ given in (3.11), one can obtain similar results of the amplitude and the phase skewing of the stationary output signals

$$S=F\left|\hat{G}_{10}\left(i\Omega\right)\right|,\quad \vartheta=\arg\left(\hat{G}_{10}\left(i\Omega\right)\right), \tag{3.13}$$

through calculation the steady-state output amplitude can be expressed as follows

$$S=FG\,,\quad G=\sqrt{\frac{g_1^{\ 2}+g_2^{\ 2}}{g_3^{\ 2}+g_4^{\ 2}}}\quad \vartheta=\arctan\left(\frac{g_2g_3-g_1g_4}{g_1g_3+g_2g_4}\right), \tag{3.14}$$

G represents the output amplitude gain (OAG) of the response, S^2 is sometimes called the spectral amplification[45]. coefficients g_k, $k=1,\ldots,4$ are expressed by

$$g_1=\omega_0^{\ 2}+r^2\cos\left(2\theta\right)+\left(\delta+\Lambda E_\alpha+E_\beta\right)r^q\cos\left(q\theta\right),\quad g_2=r^2\sin\left(2\theta\right)+\left(\delta+\Lambda E_\alpha+E_\beta\right)r^q\sin\left(q\theta\right)$$

$$\begin{aligned}g_3&=\omega_0^{\ 4}-\omega_0^{\ 2}\Omega^2+\omega_0^{\ 2}\Omega^q\left(\delta+E_\beta\right)\cos\left(\pi q/2\right)+r^2\left(\omega_0^{\ 2}-\Omega^2\right)\cos\left(2\theta\right)\\&+r^q\left(\omega_0^{\ 2}-\Omega^2\right)\left(\delta+\Lambda E_\alpha+E_\beta\right)\cos\left(q\theta\right)+r^2\Omega^q\left(\delta+E_\beta\right)\cos\left(2\theta+\pi q/2\right)\\&+r^q\Omega^q\left[\left(\delta+E_\beta\right)\left(\delta+\Lambda E_\alpha+E_\beta\right)-\sigma E_\alpha^{\ 2}\right]\cos\left[\left(\pi/2+\theta\right)q\right]\end{aligned}$$

$$\begin{aligned}g_4&=\omega_0^{\ 2}\Omega^q\left(\delta+E_\beta\right)\sin\left(\pi q/2\right)+r^2\left(\omega_0^{\ 2}-\Omega^2\right)\sin\left(2\theta\right)\\&+r^2\Omega^q\left(\delta+E_\beta\right)\sin\left(2\theta+\pi q/2\right)+r^q\left(\omega_0^{\ 2}-\Omega^2\right)\left(\delta+\Lambda E_\alpha+E_\beta\right)\sin\left(q\theta\right)\\&+r^q\Omega^q\left[\left(\delta+E_\beta\right)\left(\delta+\Lambda E_\alpha+E_\beta\right)-\sigma E_\alpha^{\ 2}\right]\sin\left[\left(\pi/2+\theta\right)q\right]\end{aligned}$$

$$r=b_1=\sqrt{v^2+\Omega^2}\,,\quad \theta=\theta_1=\arctan\left(\frac{\Omega}{v}\right).$$

4. Diverse stochastic resonances

There are many indicators to measure the degree of stochastic resonance, e.g., as the earliest measure, signal-to-noise ratio (SNR) is defined as the ratio of the power spectrum at the corresponding signal frequency to the average power spectrum of background noise. Another method is residence time characterization method[46], which measures SR in a symmetric bistable system by calculating the average residence time of particles in a potential well of the system. In this paper measurement method proposed by Gitterman is adopted[45], say, steady-state output amplitude S (or SPA S^2), to measure the SR effect degree.

4.1. SR induced by σ

When considering the effect of dichotomous noise on SR of system (1.11), the critical result of analytical expression (3.14) obtained in Section 3 can be utilized to give the theoretical analysis of SR. S depends entirely on the inherent frequency ω_0^2, excitation frequency Ω, damping strength δ, damping order q of the system, as well as the switching rate v of asymmetric double-valued color noise and related index coefficients Λ, E_α and E_β. For the convenience of calculation, the amplitude of the external excitation is assumed as $F=1$, then $S=G$ in the following analysis.

Fig. 3 shows the variation of S as a function of noise intensity under different damping orders. According to Sec. 2, when the transition rate per unit of time from Δ_1 to $-\Delta_2$ (and the opposite direction) are fixed, it can thus be seen from $D=\sigma/v$ that the noise intensity depends entirely on σ. In Fig. 3 the spectral amplification of the system exhibit nonlinearity with respect to σ for both the case of $q=1.4$ and $q=1.8$, thus the collective SR gets confirmation in the coupled oscillator. Different fractional damping orders have a significant effect on the critical noise intensity corresponding to the optimal point of SR. That is, when other parameters fixed and the damping order varies, a larger value of damping order will promote the occurrence of collective SR induced by noise intensity. In addition, no SR phenomenon occurs for $0<q<1$, but occurs for $1<q<2$. which also confirms that important novel dynamics phenomenon may be missed if only discuss the damping order below 1 [47]. In order to explained this from a more intuitive point of view, the dependency graph of system SPA on joint parameters (q,σ) is plotted in Fig. 3(b). The SR phenomenon only appears when the noise intensity is small and the damping order q near 2. On the one hand, it shows that appropriate noise intensity can enhance the synergistic effect of periodic signal and random factor. On the other hand, the damping force of the system increases with the damping order increases from 1 to 2, the energy required to drive the particle to cross the potential barrier is larger than that for $q<1$. Indeed, using the analytical formula (3.14), one can obtain the critical value σ_{SR} which corresponds to the optimal SPA peak of SR, by solving the equation $\mathrm{d}S(\sigma)/\sigma=0$. The equivalent equation is $g_3\,\partial g_3/\partial\sigma+g_4\,\partial g_4/\partial\sigma=0$, then the extreme noise intensity σ_{SR} is given by

$$\sigma_{SR}=\frac{1}{r^q\Omega^q E_\alpha{}^2}\Big\{\left(\omega_0{}^4-\omega_0{}^2\Omega^2\right)\cos\left[\left(\frac{\pi}{2}+\theta\right)q\right]+\omega_0{}^2\Omega^q\left(\delta+E_\beta\right)\cos\left(\theta q\right)$$
$$+r^2\left(\omega_0{}^2-\Omega^2\right)\cos\left[\frac{\pi q}{2}+\left(q-2\right)\theta\right]+r^q\left(\omega_0{}^2-\Omega^2\right)\left(\delta+\Lambda E_\alpha+E_\beta\right)\cos\left(\frac{\pi q}{2}\right), \quad (4.1)$$
$$+r^2\Omega^q\left(\delta+E_\beta\right)\cos\left[\left(2-q\right)\theta\right]+r^q\Omega^q\left(\delta+E_\beta\right)\left(\delta+\Lambda E_\alpha+E_\beta\right)\Big\}$$

if substituting the critical noise intensity σ_{SR} into Equation (3.14), one can obtain the optimal maximum of SPA when SR occurs.

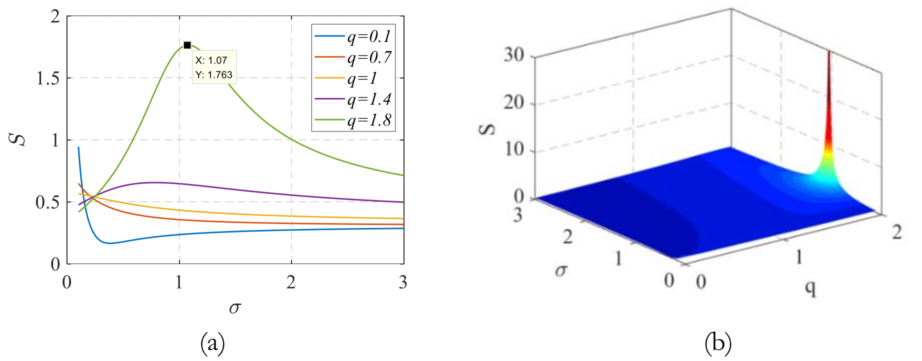

Fig. 3. (Color online) (a) Output amplitude S versus noise intensity under different values of fractional order q. (b) Dependence of output amplitude on joint parameters (q,σ). Other parameters are $\varepsilon=0.8$, $\delta=0.5$, $E_\alpha=1.9$, $E_\beta=0.3$, $\omega_0{}^2=1$, $\Omega=1.5$, $v=0.01$, $\Delta_1=2\Delta_2$.

As the inherent frequency $\omega_0{}^2$ is included in the analytical result (3.14), it is necessary to examine its influence on collective traditional SR induced by σ. In addition, according to the stability condition (3.10), $\omega_0{}^2$ will also affect the stability of steady-state output amplitude results, one can obtain the *stability condition* with respect to $\omega_0{}^2$ as

$$\omega_0{}^2>\omega_{0cr}{}^2=-v^2-\left(\delta+\Lambda E_\alpha+E_\beta\right)v^q, \quad (4.2)$$

wherein $\omega_{0cr}{}^2$ is refer as *critical intrinsic frequency*. Consider the system parameters $\varepsilon=0.8$, $\delta=0.5$, $E_\alpha=1.9$, $E_\beta=0.3$, $\omega_0{}^2=1$, $\Omega=1.5$, $v=0.01$, $\Delta_1=2\Delta_2$, Fig. 4 shows the influence of different $\omega_0{}^2$ values on collective SR under different damping orders ($q=0.5, 1, 1.5$). It can be seen that the steady-state output amplitude increases with the increase of $\omega_0{}^2$ under each case, while it only peaks for $q=1.5$. Moreover, a comparation of the three curves in Fig. 4(c) shows that the resonance peak value $S_{\max}\left(\sigma_{SR}\right)$ increases with the increase of the inherent frequency. In fact, for the system without noise disturbance corresponding to system (1.11), the mean field of the deterministic system has a potential function of harmonic form $U\left(z\right)=\omega_0{}^2z/2$, wherein the parameter $\omega_0{}^2$ denotes potential intensity. The potential function becomes narrower when $\omega_0{}^2$ increases, so the oscillator has to reach a higher oscillation range under the same amplitude condition, results in a larger steady-state amplitude. Under the synergy of dichotomous colored noise, coupled system and periodic excitation, a narrower potential does not require a larger noise intensity to drive the oscillator approaching the optimal oscillation amplitude point. This reveals the mechanical mechanism why the critical noise intensity σ_{SR} decreases with the increase of $\omega_0{}^2$.

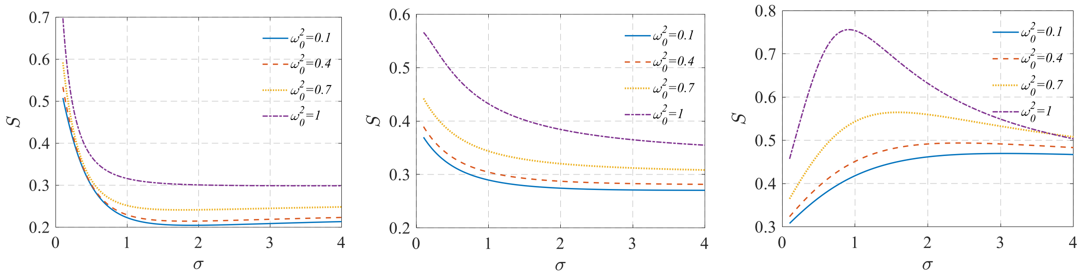

(a) (b) (c)

Fig. 4. (Color online) Effect of the intrinsic frequency on SR induced by σ. (a) $q = 0.5$; (b) $q = 1$ (b) $q = 1.5$.

4.2. Bona Fide SR

The Bona fide SR indicates the peak phenomenon of output signal amplitude induced by the fluctuation of signal frequency[48]. Before a detail discussion of the possible existence of Bona fide SR phenomena in the system (1.11) that may be induced by external excitation frequency, we first consider the corresponding deterministic version (i.e.， $E_\alpha = E_\beta = 0$)

$$\begin{cases} \ddot{z}_1(t) + \delta\,\mathrm{D}^q\, z_1(t) + \omega_0{}^2 z_1(t) = \varepsilon(z_2 - z_1) + F\cos(\Omega t) \\ \ddot{z}_2(t) + \delta\,\mathrm{D}^q\, z_2(t) + \omega_0{}^2 z_2(t) = \varepsilon(z_1 - z_2) + F\cos(\Omega t) \end{cases}. \tag{4.3}$$

Further simplification leads to an equation for the mean field

$$\ddot{z}(t) + \delta\,\mathrm{D}^q\, z(t) + \omega_0{}^2 z(t) = F\cos(\Omega t),$$

the solution $z(t) = A^*\cos(\Omega t + \phi)$ of the equation can be obtained by using the method of undetermined coefficients, with the amplitude given by

$$A^* = \frac{F}{\sqrt{\left(\Omega^2 - \omega_0{}^2 - \delta\Omega^q\cos(\pi q/2)\right)^2 + \left(\delta\Omega^q\sin(\pi q/2)\right)^2}}, \tag{4.4}$$

phase angle is $\phi = \tan^{-1}\left[\delta\Omega^q\sin(\pi q/2)/\left(\Omega^2 - \omega_0{}^2 - \delta\Omega^q\cos(\pi q/2)\right)\right]$. In addition, the same results can be obtained when inserting $E_\alpha = E_\beta = 0$ into (3.14)， which indicates that system (4.3) is actually a special case of system (1.11).

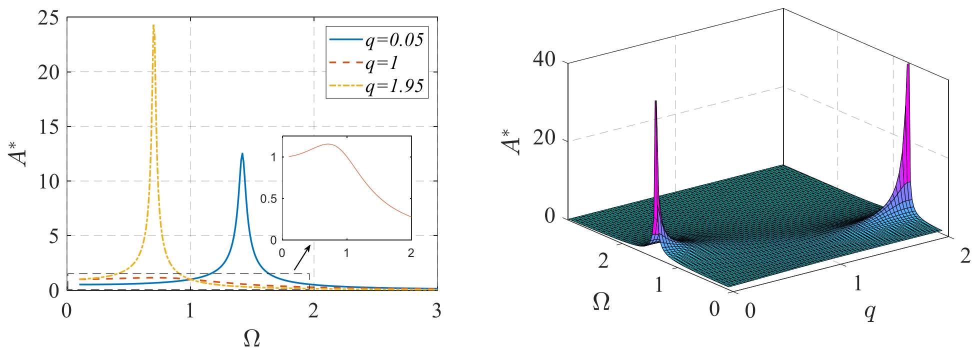

(a) (b)

Fig. 5. (Color online) (a) Output amplitude of system (4.3) versus excitation frequency Ω under different fractional order. (b) Analytical result of A^* versus Ω and q according to Eq. (4.4)

Consider the system parameters $F = 1$, $\delta = 1$, $\omega_0 = 1$, the influence of external excitation frequency on output amplitude A^* under different damping orders has been plotted in Fig. 5(a). It can be seen that as a function of Ω, A^* exhibits SR-like non-monotonicity in all three cases. It is noteworthy that the resonance degree of fractional cases $q=0.05$ and $q=1.95$ are more striking than that of integer order. The introduction of fractional damping order brings about new resonance behavior, and under same parametric condition, Bona fide SR is more likely to occur in the fractional case. It is observed that the optimal peak point occurs at $q=1.95$, once again proving the necessity of considering the damping order $1<q<2$. Fig. 5(b) shows the combined effect of Ω and damping order on output amplitude A^*. The Single-resonance point Ω_R always exists and gradually increases with the increase of q, while the peak firstly decreases and then increases, and gets unobtrusive when q approaches the integer-case. Indeed，the critical frequency corresponds to the peak satisfies $\mathrm{d}A^*(\Omega)/\mathrm{d}\Omega=0$. For $q\to 0$, it can be obtained from the (4.4) that $A^*\to F/\left|\Omega^2-\omega_0^{\,2}-\delta\right|$, the corresponding frequency is given by $\Omega_R=\sqrt{\omega_0^{\,2}+\delta}$. The single-peak SR will certainly emerge and $A^*_{\max}\to\infty$ when $q\to 0$, which can explain why a saltation within a certain frequency range appears in the figure. The system (4.3) would be reduced to the deterministic integer-order version for $q=1$, and the output amplitude reads $A^*=F\Big/\sqrt{\left(\Omega^2-\omega_0^{\,2}\right)^2+\delta^2\Omega^2}$ with the critical frequency calculated by $\Omega_R=\sqrt{\omega_0^{\,2}-\delta^2/2}$. Then the resonance peak point with the optimal value $A_R^*=2F\Big/\left(\delta\sqrt{4\omega_0^{\,2}-\delta^2}\right)$ will appear when the parametric condition $\delta<\sqrt{2}\omega_0$ is met. When inserting the limit setting $q\to 2$ into (4.4) one gets $A^*\to F/\left|(1+\delta)\Omega^2-\omega_0^{\,2}\right|$ and $\Omega_R=\sqrt{\omega_0^{\,2}/(1+\delta)}$, that's why another saltation appears at frequency $\Omega=0.7$ in Fig. 5(a). The peak values of the three cases in the figure are consistent with the above analysis results, respectively.

When considering the presence of color noise disturbance, the transfer rate ν is sometimes called the correlation rate, which reflects the memory effect of noise. In order to facilitate the analysis, the possible SR results under the slow switching $(\nu\to 0)$ and fast switching $(\nu\to\infty)$ patterns of asymmetric dichotomous noise will be examined respectively. The switching rate between states Δ_1 and $-\Delta_2$ will be extremely slow for a small correlation rate, which leads to an excessive correlation time. In fact, a state transition of the colored noise will be accompanied by a long-time stagnation, the damping strength can actually be seen be fixed during this period. Accordingly, in this case random damping disturbance coefficient in (1.11) can be divided into two cases in quite long time

$$\delta+\Phi(\eta(t),N)=\begin{cases}\delta+E_\alpha\Delta_1+E_\beta\\ \delta-E_\alpha\Delta_2+E_\beta\end{cases}. \tag{4.5}$$

For a long time before the next jump of noise, (1.11) can be regarded as deterministic system whose damping strength is either of the two in (4.5), so the delta in (4.4) can be replaced. Based on the resonance extremum condition $\mathrm{d}A^*(\Omega)/\mathrm{d}\Omega=0$, it can be estimated that when $q\to 0$, double-peak SR induced by frequency Ω may appear at critical frequencies

$$\Omega_{SR1}\approx\sqrt{\omega_0^{\,2}+\delta+E_\alpha\Delta_1+E_\beta}\,,\qquad \Omega_{SR2}\approx\sqrt{\omega_0^{\,2}+\delta-E_\alpha\Delta_2+E_\beta}\,.$$

which is indeed consistent with the two peak points 0.4 and 2.44 corresponding to the noise intensity $\sigma=2.2$ (i.e., $\Delta_2=1.1$) in Fig. 6(a), so the bimodal Bona Fide SR induced by the external excitation frequency is confirmed. The value of noise state Δ_2 is too large for $\sigma=3$ and $\sigma=3.6$, leading to $\omega_0^2+\delta-E_\alpha\Delta_2+E_\beta<0$, that SR with one peak happens at Ω_{SR1}. When $q=1$, all possible critical resonance frequencies corresponding to SR can also be calculated in an analogical way, given as

$$\Omega_{SR1}\approx\sqrt{\omega_0^2-\left(\delta+E_\alpha\Delta_1+E_\beta\right)^2/2}\,,\qquad \Omega_{SR2}\approx\sqrt{\omega_0^2-\left(\delta-E_\alpha\Delta_2+E_\beta\right)^2/2}\,.$$

When $q\to2$, all the two possible resonance positions become

$$\Omega_{SR1}\approx\sqrt{\omega_0^2/\left(1+\delta+E_\alpha\Delta_1+E_\beta\right)}\,,\qquad \Omega_{SR2}\approx\sqrt{\omega_0^2/\left(1+\delta-E_\alpha\Delta_2+E_\beta\right)}\,.$$

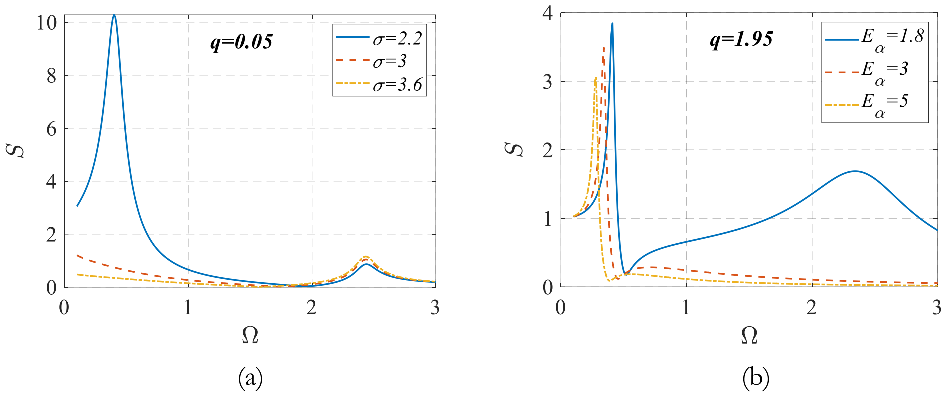

Fig. 6. (Color online) Dependence of SPA on noise intensity and parameter under slow-switching noise situation. (a) $q=0.05$, $\Delta_2=1.1,1.5,1.8$; (b) $q=1.95$. Other system parameters are $\varepsilon=0.5$, $\delta=0.7$, $E_\beta=0.4$, $\omega_0^2=1$, $F=1$, $v=0.01$ $\Delta_1=2$.

these analyses match the position 0.41 and 2.32 of two resonant peaks corresponding to noise intensity $E_\alpha=1.8$, accompanying with the occurrence of double-peak SR in Fig. 6(b). For larger noise coefficients $E_\alpha=3$ and $E_\alpha=5$, $1+\delta-E_\alpha\Delta_2+E_\beta<0$ thus single-resonance occurs at Ω_{SR1}. A remarkable thing is that for $q=1.95$, the steady-state output amplitude exhibits a saltation near $\Omega=0.4$, which is analogous to hypersensitivity response[49]. That is, a slight change in frequency will result in a dramatic change in steady-state output amplitude within a very small frequency range.

In the case of fast switching noise, the steady-state output amplitude can be estimated according to (3.14)

$$A=\frac{F}{\sqrt{\left[\omega_0^2-\Omega^2+\Omega^q\left(\delta+E_\beta\right)\cos\left(\pi q/2\right)\right]^2+\left[\Omega^q\left(\delta+E_\beta\right)\sin\left(\pi q/2\right)\right]^2}}\,,\qquad(4.6)$$

combining with (4.6) and (4.4), the result of (4.6) just corresponds to the steady-state solution amplitude of the following deterministic system

$$\ddot{z}(t)+\delta^*\,\mathrm{D}^q\,z(t)+\omega_0^2 z(t)=F\cos(\Omega t)\,,\qquad(4.7)$$

with the equivalent damping strength $\delta^*=\delta+E_\beta$. For $q\to0$, from (4.6) one gets $\Omega_{SR}=\sqrt{\omega_0^2+\delta+E_\beta}$, thus Bona Fide SR always exist within the range of parameters considered, which is consistent with the critical frequency values at the peak point 1.41 as shown in Fig. 7. For the integer-order damping case $q=1$, $\Omega_{SR}=\sqrt{\omega_0^2-\left(\delta+E_\beta\right)^2/2}$ holds under the condition $\omega_0^2-\left(\delta+E_\beta\right)^2/2>0$. The critical frequency corresponding to single-peak SR can also be estimated as $\Omega_{SR} \approx \sqrt{\omega_0^2/(1+\delta+E_\beta)}$ when q approaching to 2. Accordingly, compared with the integer order case, the conditions for the occurrence of SR in the other two cases of fractional order damping are much looser. In other words, the phenomena of Bona fide SR are more likely to occur in the fractional case. Fixing system parameters at $\varepsilon=0.5$, $\delta=0.7$, $E_\alpha=1.8$, $E_\beta=0.4$, $\omega_0^2=1$, $F=1$, $\Delta_1=2$, $\Delta_2=1.1$, Fig. 7 shows the single-peak Bona fide SR under the fast-switching noise situation ($v=8$), wherein the peaks are consistent with the above analysis.

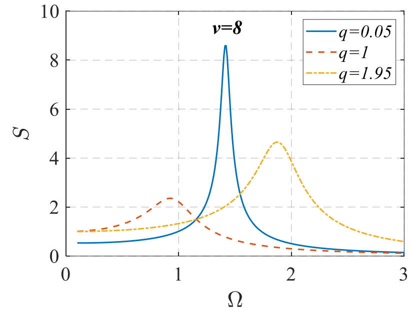

Fig. 7. (Color online) Dependence of output steady-state amplitude on excitation frequency under $q=0.05$, $q=1$ and $q=1.95$ with fast-switching noise.

Fig. 8 shows the single- and double-peak Bona Fide SR with different noise switching rates. For a slow switching rate, the system will be equivalent to the case of two deterministic systems with damping strength of $\delta+E_\alpha\Delta_1+E_\beta$ or $\delta-E_\alpha\Delta_2+E_\beta$ in A long correlation time, so that the double-peak SR phenomenon will happen. As v increases, jumps of the noise between two states become more and more frequently, two resonant peaks gradually converge and eventually merged into the only one. In order to explain this phenomenon intuitively, the phase diagram of Bona Fide SR depending on joint parameters (q,v) is given in Fig. 8(c), it is found that bimodal SR only occurs when the damping order is close to 0 or 2. Moreover, for cases of $v>0.74$ with small q or $v>0.93$ with large q, the variation of Ω can only induce at most one peak of the steady-state output amplitude.

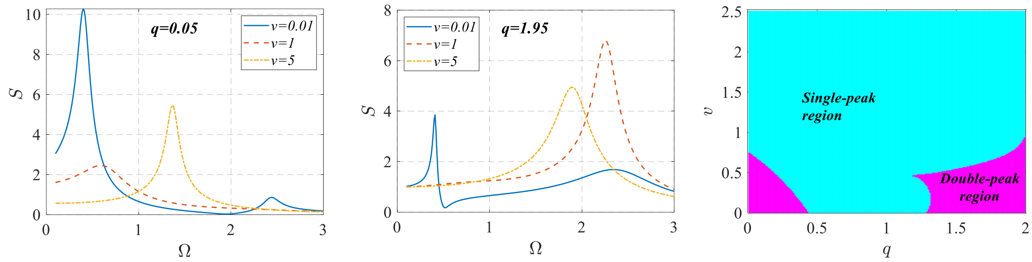

(a) (b) (c)

Fig. 8. (Color online) Effect of noise switching rate on the output steady-state amplitude. (a) $q=0.05$; (b) $q=1.95$; (c) Cyan area corresponds to single-peak SR and rosy red area corresponds to double-peak SR. Other parameters are $\varepsilon=0.5$, $\delta=0.7$, $E_\alpha=1.8$, $E_\beta=0.4$, $\omega_0^2=1$, $F=1$, $\Delta_1=2$, $\Delta_2=1.1$.

4.3. SR in broad sense

SR in broad sense[50] proposed by Gitterman refers to the non-monotonic dependence of some functions of the output signal (such as SNR, autocorrelation function, amplitude gain, etc.) on noise or system parameters, showing that traditional SR is actually included in the concept of generalized stochastic resonance (GSR).

When other parameters in the system are fixed while the damping strength varying, the steady-state output amplitude of the output signal is regarded as a function of δ, here we examine whether the variation of δ will bring about the nonlinear peak phenomenon, i.e., whether GSR exists. Firstly, consider the slow-switching noise（$v \to 0$）, In the process of each state switch of noise, the damping strength of the system can be approximately regarded as deterministic, given in (4.5). Substitute the two cases in (4.5) into (4.4) and solve the equation of resonance extremum condition $\mathrm{d}A^*(\delta)/\mathrm{d}\delta = 0$, one gets all the possible analytical results of critical damping strength when resonance occurs

$$\begin{cases} \delta_{SR1} = \left(\Omega^{2-q} - \omega_0^2\Omega^{-q}\right)\cos\left(q\pi/2\right) - E_\alpha\Delta_1 - E_\beta \\ \delta_{SR2} = \left(\Omega^{2-q} - \omega_0^2\Omega^{-q}\right)\cos\left(q\pi/2\right) + E_\alpha\Delta_2 - E_\beta \end{cases}, \tag{4.8}$$

Fig. 9 presents some theoretical curves of GSR induced by variation of damping strength under different damping order (Fig. 9(a)) and different natural frequency (Fig. 9(b)). Double-peak pattern of GSR is confirmed in left diagram for $q = 0.1$. Steady-state output amplitude function peaks at 0.6 and 2.27 with the increase of δ, while only peak once at 1.25 when damping order equals 0.3, this is because $\delta_{SR1} < 0$ for $q = 0.3$ and only δ_{SR2} exists. Both the values of δ_{SR1} and that of δ_{SR2} are negative for $q = 1$ and $q = 1.5$, wherein the damping strength cannot induce any kind of GSR. Something similar happens when consider the effect of different inherent frequency, as shown in Fig 9(b). $\delta_{SR1} < 0$ for $\omega_0^2 = 2$ and the only single-peak point appears at the second predicted value $\delta_{SR2} = 0.56$. According to the above analysis, one can make further predictions that no SR will cease to exist when the inherent frequency is too large.

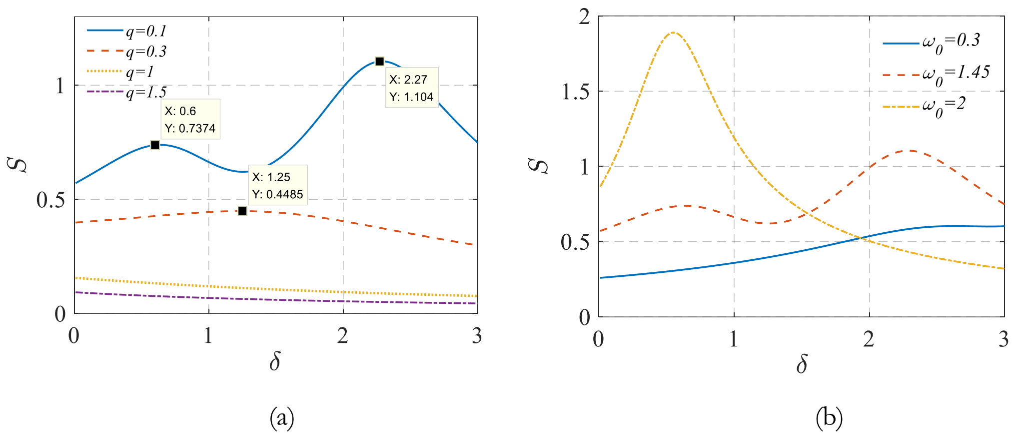

Fig. 9. (Color online) Damping strength inducing GSR with slow-switching noise. (a) $\omega_0^2 = 1.45$; (b) $q = 0.1$. Other parameters are $\varepsilon = 0.5$, $E_\alpha = 0.5$, $E_\beta = 2$, $\Omega = 2.5$, $\Delta_1 = 2$, $\Delta_2 = 1$, $v = 0.01$.

When the dichotomous noise is in fast-switching mode, Fig. 10(a) shows the dependence of steady-state output amplitude on damping strength under different damping orders. GSR only occurs at $\delta_{SR} = 1.74$ for $q = 0.1$, while decreases gradually with the increase of δ in the other two cases. Indeed, a theoretical analytical estimate can still be conducted by virtue of formula (4.6) and the extremal condition equation $\mathrm{d}A^*(\delta)/\mathrm{d}\delta = 0$, the only possible critical damping strength expression when resonance occurs can be expressed as

$$\delta_{SR} = \left(\Omega^{2-q} - \omega_0^{\,2}\Omega^{-q}\right)\cos\left(q\pi/2\right) - E_\beta, \tag{4.9}$$

(4.9) is very similar to (4.8) in form, which corresponds to the peak point of the solid blue curve in Fig.10 (a), and negative results will be obtained either $q = 0.5$ or $q = 1.5$ is inserted into (4.9), so the optimal value does not exist. In addition, GSR induced by δ under different noise parameters E_β has been examined in FIG. 10(b). It is not difficult to find that variation of E_β can only change the SR location, but not make any influence on the peak value of optimal output amplitude.

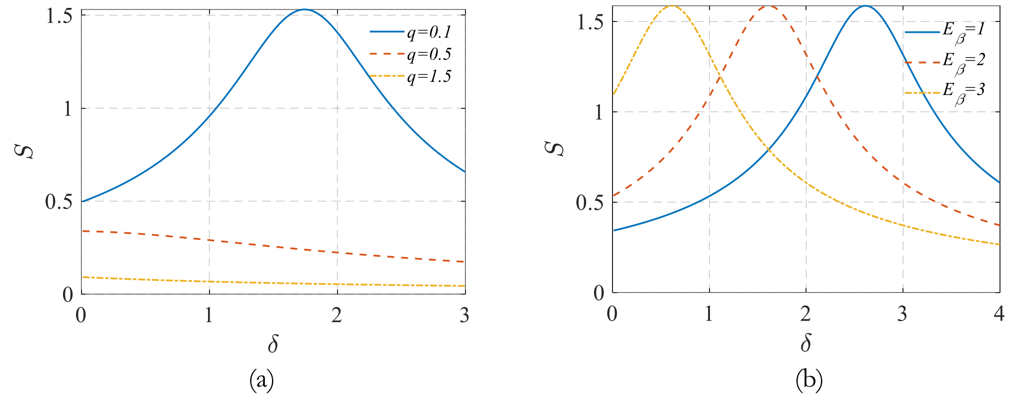

Fig. 10. (Color online) Damping strength inducing GSR with fast-switching noise. (a) $E_\beta = 2$; (b) $q = 0.1$. Other parameters are $\varepsilon = 0.5$, $E_\alpha = 0.5$, $\Omega = 2.5$, $\Delta_1 = 2$, $\Delta_2 = 1$, $\omega_0^{\,2} = 1.5$, $v = 8$.

By substituting (4.9) into (4.6), one can estimate the analytical prediction expression of the peak value of output amplitude of the system as

$$A \approx \frac{F}{\left|\left(\Omega^2 - \omega_0^{\,2}\right)\sin\left(q\pi/2\right)\right|}, \tag{4.10}$$

this prediction result is consistent with the single peak value result $A_{opt} = 1.587$ in FIG. 10(b)

At last based on above, it is not difficult to realize that due to the introduction of fractional damping in the coupled system, the fractional damping order have a significant impact on the phenomena of GSR induced by system parameters. When it is regarded as the only control variable, the steady-state output amplitude S is a complex function containing q, it is difficult to directly calculate the concrete explicit expression of the critical value of fractional damping order, say, q_{SR}. Nonetheless, one can still provide the dependence relation between the output response of the system and q from a numerical estimation point of view. Considering parameters $\varepsilon = 0.5$, $E_\alpha = 1$, $E_\beta = 1$, $\delta = 2$, $\Omega = 2.5$, $\Delta_1 = 2$, $\Delta_2 = 1$, $\omega_0^{\,2} = 1.5$, S versus controlled parameter q under different degree of noise switching rate are shown in Fig. 11(a). It finds that under appropriate parameter conditions, GSR phenomenon can indeed be produced by controlling the damping order. According to the trend of the joint dependence of system response on parameters (q, v) in Fig.11 (b), it can be determined that smaller damping order and larger noise switching rate are more conducive to the occurrence of stronger SR phenomenon of the system, this new finding is different from the previous conclusions[51]. Comparing to the situation where the colored noise is regarded as the mass disturbance of the oscillator, noises' switching rate has a more significant effect on the SR behavior of the system when it is regarded as the damping disturbance.

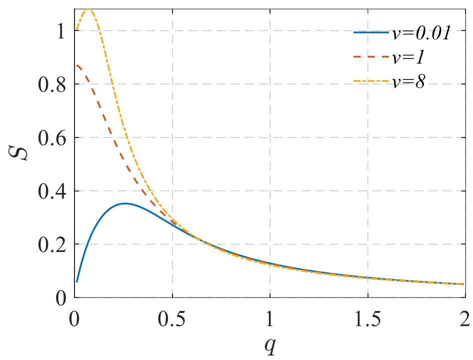

(a)

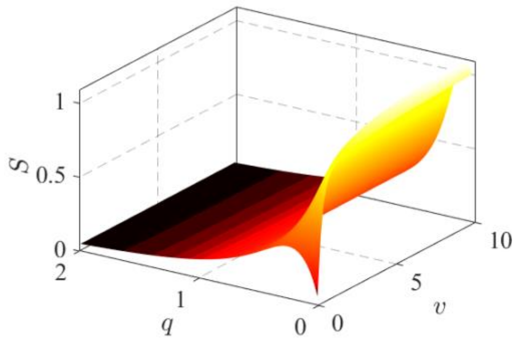

(b)

Fig. 11. (Color online) (a) GSR induced by the order of fractional damping with different switching rate. (b) Dependence of out steady-state amplitude on damping order and switching rate.

5. Conclusion

In this present study, several kinds of SR phenomena in coupled stochastic fractional oscillator systems are studied, which endures external periodic signal and damping disturbance of asymmetric dichotomous noise of polynomial form. The utilization of averaging method is developed by employing the fractional Shapiro-Loginov formula and fractional Laplace transformation law. Theoretical results of steady-state output amplitude of the coupled system as well as the first moment of the system response relying on stochastic vibrational Mechanism are obtained. Based on which phenomena of traditional SR induced by noise intensity, Bona fide SR induced by external excitation frequency and GSR induced by different system parameters are discussed in detail, respectively. Moreover, in order to understand the stochastic resonance phenomenon in a more intuitional way, we give the parametric phase diagram of the output amplitude, and explain the mechanism of different stochastic resonance.

The analytical results provide a convenient and shortcut approach to reveal the mechanism of two kinds of stochastic resonance. When examining SR induced by noise intensity, we determine the significant effect of fractional damping order on the system. In the case that the noise states satisfy $\Delta_1 = 2\Delta_2$, it is found that SR only occurs when the damping order is close to 2, indicating the necessity to consider the damping case $q < 2$ in the fractional order. The explicit analytical expression of the critical dichotomous noise intensity corresponding to the optimal peak point is obtained, and it is proved that synergy between periodic signal and random factor in the system can be enhanced by appropriate noise intensity. It is found that Bona fide SR is more likely to happen in the fractional order case than in the integer-one case, and a stronger degree of SR usually doesn't correspond to a larger noise intensity. A comparison between the deterministic system and stochastic one releases that the addition of dichotomous noise brings about new resonance behaviors in the system (Fig. 6). In addition, In the slow-switching noise case, a newfangled phenomenon of hypersensitive response excitation frequency is discovered, by which a novel fact has been validated and confirmed that the polynomial dichotomous noise does induce a new dynamic behavior, which has not been reported in previous work. By means of the phase diagram of the system depending on damping order and noise switching rate, it is found that bimodal SR occurs only in the parameter region with slow switching noise and damping order close to 0 or 2 (Fig.8 (c)). The results of GSR indicate that when damping strength is considered as the controlled parameter, multimodal GSR happens only for the colored noise with slow switching rate (Fig. 9), which is reported for the first time. Moreover, it is determined that not only the parameters of the colored noise but also the inherent frequency can induce different GSR patterns, as shown in Fig. 9(b) and Fig. 10(b). It can be determined that damping order has a significant effect on the GSR induced by damping strength. These analyses guarantee that the system response can be controlled effectively by selecting appropriate parameters. It is believed that the methods developed and the results obtained in this paper, is meaningful in further investigating in coupled stochastic fractional systems. Relevant findings and discussions are useful for dealing with some real fractional order issues, and shed new light on the studies of dynamical behavior disturbed by nonlinear color noise.

Funding

This work was supported by National Natural Science Foundation of China (No.12002194; No.12072178); Project No.ZR2020MA054 supported by Shandong Provincial Natural Science Foundation.

Data Statement: Data sharing not applicable to this article as no datasets were generated or analysed during the current study.

Conflict of Interest: The authors declare that they have no conflict of interest.

References

[1] Xu P, Jin Y. Stochastic resonance in multi-stable coupled systems driven by two driving signals. Physica A: Statistical Mechanics and Its Applications, 2018, 492: 1281-1289.

[2] Bi H, Lei Y, Han Y. Stochastic resonance across bifurcations in an asymmetric system. Physica A: Statistical Mechanics and its Applications, 2019, 525: 1296-1312.

[3] Silva I G, Korneta W, Stavrinides S G, et al. Observation of stochastic resonance for weak periodic magnetic field signal using a chaotic system. Communications in Nonlinear Science and Numerical Simulation, 2021, 94: 105558.

[4] Wu C, Lv S, Long J, et al. Self-similarity and adaptive aperiodic stochastic resonance in a fractional-order system. Nonlinear Dynamics, 2018, 91(3): 1697-1711.

[5] Xu Y, Guo Y, Ren G, et al. Dynamics and stochastic resonance in a thermosensitive neuron. Applied Mathematics and Computation, 2020, 385: 125427.

[6] Zhang G, Shi J, Zhang T. Stochastic resonance in an under-damped linear system with nonlinear frequency fluctuation. Physica A: Statistical Mechanics and its Applications, 2018, 512: 230-240.

[7] Mondal S, Das J, Bag B C, et al. Autonomous stochastic resonance driven by colored noise. Physical Review E, 2018, 98(1): 012120.

[8] Aghili A. Complete solution for the time fractional diffusion problem with mixed boundary conditions by operational method. Applied Mathematics and Nonlinear Sciences, 2021, 6(1): 9-20.

[9] Singh J, Ganbari B, Kumar D, et al. Analysis of fractional model of guava for biological pest control with memory effect. Journal of Advanced Research, 2021, 32: 99-108.

[10] Qi X, Li H, Chen B, et al. A prediction model of urban counterterrorism based on stochastic strategy. Applied Mathematics and Nonlinear Sciences, 2021, 6(1): 263-268.

[11] Failla G, Zingales M. Advanced materials modelling via fractional calculus: challenges and perspectives. Philosophical Transactions of the Royal Society A, 2020, 378(2172): 20200050.

[12] Feddaoui A, Llibre J, Berhail C, et al. Periodic solutions for differential systems in ℝ 3 and ℝ 4. Applied Mathematics and Nonlinear Sciences, 2021, 6(1): 373-380.

[13] Shen L J. Fractional derivative models for viscoelastic materials at finite deformations. International Journal of Solids and Structures, 2020, 190: 226-237.

[14] Evangelista L R, Lenzi E K. Fractional diffusion equations and anomalous diffusion. Cambridge University Press, 2018.

[15] Haque B M I, Flora S A. On the analytical approximation of the quadratic non-linear oscillator by modified extended iteration method. Applied Mathematics and Nonlinear Sciences, 2021, 6(1): 527-536.

[16] Varanis M V, Tusset A M, Balthazar J M, et al. Dynamics and control of periodic and non-periodic behavior of Duffing vibrating system with fractional damping and excited by a non-ideal motor. Journal of the Franklin Institute, 2020, 357(4): 2067-2082.

[17] Cinlar E. Introduction to stochastic processes. Courier Corporation, 2013.

[18] Wang B. Dynamics of fractional stochastic reaction-diffusion equations on unbounded domains driven by nonlinear noise. Journal of Differential Equations, 2019, 268(1): 1-59.

[19] Zhang L, Zhong S C, Peng H, et al. Stochastic multi-resonance in a linear system driven by multiplicative polynomial dichotomous noise. Chinese Physics Letters, 2011, 28(9): 090505.

[20] Kaur D, Agarwal P, Rakshit M, et al. Fractional Calculus involving (p, q)-Mathieu Type Series. Applied Mathematics and Nonlinear Sciences, 2020, 5(2): 15-34.

[21] Boccaletti S, Pisarchik A N, Del Genio C I, et al. Synchronization: from coupled systems to complex networks. Cambridge University Press, 2018.

[22] Touchent K A, Hammouch Z, Mekkaoui T. A modified invariant subspace method for solving partial differential equations with non-singular kernel fractional derivatives. Applied Mathematics and Nonlinear Sciences, 2020, 5(2): 35-48.

[23] Caponetto R. Fractional order systems: modeling and control applications. Singapore: World Scientific, 2010.

[24] Yan Z, Wang W, Liu X B. Analysis of a quintic system with fractional damping in the presence of vibrational resonance. Appl, Math Comput, 2018, 321: 780-793

[25] Fang Y, Luo Y, Zeng C. Dichotomous noise-induced negative mass and mobility of inertial Brownian particle. Chaos, Solitons & Fractals, 2022, 155: 111775.
[26] Moshe Gitterman, Oscillator with random mass, World Journal of Mechanics, 2012, 2: 113-124.
[27] Kanna M R R, Kumar R P, Nandappa S, et al. On solutions of fractional order telegraph partial differential equation by Crank-Nicholson finite difference method. Applied Mathematics and Nonlinear Sciences, 2020, 5(2): 85-98.
[28] Fang Y, Luo Y, Zeng C. Dichotomous noise-induced negative mass and mobility of inertial Brownian particle. Chaos, Solitons & Fractals, 2022, 155: 111775.
[29] Mandrysz M, Dybiec B. Energetics of single-well undamped stochastic oscillators. Physical Review E, 2019, 99(1): 012125.
[30] Onal M, Esen A. A Crank-Nicolson approximation for the time fractional Burgers equation. Applied Mathematics and Nonlinear Sciences, 2020, 5(2): 177-184.
[31] Yang B, Zhang X, Zhang L, Luo M K. collective behavior of globally coupled Langevin equation with colored noise in the presence of stochastic resonance, Phys. Rev. E. 94, 022119 (2016).
[32] Zhong S, Lv W, Ma H, et al. Collective stochastic resonance behavior in the globally coupled fractional oscillator. Nonlinear Dynamics, 2018, 94(2): 905-923.
[33] Shapiro V E, Loginov V M. "Formulae of differentiation" and their use for solving stochastic equations. Physica A: Statistical Mechanics and its Applications, 1978, 91(3-4): 563-574.
[34] Li C P, Zeng F. Numerical methods for fractional calculus. Shanghai, CRC Press, 2015.
[35] Podlubny I. Fractional differential equations. California, Academic Press, 1999.
[36] Lynch V E, Carreras B A, del-Castillo-Negrete D, et al. Numerical methods for the solution of partial differential equations of fractional order. Journal of Computational Physics, 2003, 192(2): 406-421.
[37] Butcher J. Runge-kutta methods. Scholarpedia, 2007, 2(9): 3147.
[38] Gammaitoni L, Hänggi P, Jung P, et al. Stochastic resonance. Reviews of modern physics, 1998, 70(1): 223.
[39] Gao S L, Generalized stochastic resonance in a linear fractional system with random delay. Journal of statistical Mechanics: Theory and Experiment, 2012, 2012(12), 012011.
[40] Jarad F, Abdeljawad T. Generalized fractional derivatives and Laplace transform. Discrete & Continuous Dynamical Systems-S, 2020, 13(3): 709.
[41] Kuhfittig P K F, Introduction to the Laplace transform, Springer Science & Business Media, 2013.
[42] Kempfle S, Schäfer I, Beyer H. Fractional calculus via functional calculus: theory and applications. Nonlinear Dynamics, 2002, 29(1-4): 99-127.
[43] Luef F, Skrettingland E. A Wiener Tauberian theorem for operators and functions. Journal of Functional Analysis, 2021, 280(6): 108883.
[44] Girod B, Rabenstein R, Stenger A. Signals and Systems, Tsinghua university, Wiley 2001.
[45] Gitterman M. Classical harmonic oscillator with multiplicative noise. Physica A: Statistical Mechanics and its Applications, 2005, 352(2-4): 309-334.
[46] Escotet-Espinoza M S, Moghtadernejad S, Oka S, et al. Effect of material properties on the residence time distribution (RTD) characterization of powder blending unit operations. Part II of II: Application of models. Powder Technology, 2019, 344: 525-544.
[47] Yang J H, Sanjuán M A F, Liu H G, et al. Stochastic P-bifurcation and stochastic resonance in a noisy bistable fractional-order system. Communications in Nonlinear Science and Numerical Simulation, 2016, 41: 104-117.

[48] Gammaitoni L, Marchesoni F, Santucci S. Stochastic resonance as a bona fide resonance. Physical review letters, 1995, 74(7): 1052.

[49] Zhong S, Wei K, Gao S, et al. Trichotomous noise induced resonance behavior for a fractional oscillator with random mass. Journal of Statistical Physics, 2015, 159(1): 195-209.

[50] Huang X, Lin L, Wang H. Generalized Stochastic Resonance for a Fractional Noisy Oscillator with Random Mass and Random Damping. Journal of Statistical Physics, 2020, 178(5): 1201-1216.

[51] Tian Y, Zhong L F, He G T, et al. The resonant behavior in the oscillator with double fractional-order damping under the action of nonlinear multiplicative noise. Physica A: Statistical Mechanics and its Applications, 2018, 490: 845-856.